

Forest responses to last-millennium hydroclimate variability are governed by spatial variations in ecosystem sensitivity

Article

Accepted Version

Rollinson, C. R. ORCID: <https://orcid.org/0000-0003-0181-7293>, Dawson, A., Raiho, A. M., Williams, J. W., Dietze, M. C. ORCID: <https://orcid.org/0000-0002-2324-2518>, Hickler, T., Jackson, S. T., McLachlan, J., Moore, D. J. P., Poulter, B., Quaife, T. ORCID: <https://orcid.org/0000-0001-6896-4613>, Steinkamp, J. ORCID: <https://orcid.org/0000-0002-7861-8789>, Trachsel, M. and Morin, X. (2021) Forest responses to last-millennium hydroclimate variability are governed by spatial variations in ecosystem sensitivity. *Ecology Letters*, 24 (3). pp. 498-508. ISSN 1461-023X doi: <https://doi.org/10.1111/ele.13667> Available at <https://centaur.reading.ac.uk/96165/>

It is advisable to refer to the publisher's version if you intend to cite from the work. See [Guidance on citing](#).

To link to this article DOI: <http://dx.doi.org/10.1111/ele.13667>

Publisher: Wiley

including copyright law. Copyright and IPR is retained by the creators or other copyright holders. Terms and conditions for use of this material are defined in the [End User Agreement](#).

www.reading.ac.uk/centaur

CentAUR

Central Archive at the University of Reading

Reading's research outputs online

ECOLOGY LETTERS

Forest responses to last-millennium hydroclimate variability are governed by spatial variations in ecosystem sensitivity

Journal:	<i>Ecology Letters</i>
Manuscript ID	ELE-01100-2020.R1
Manuscript Type:	Letters
Date Submitted by the Author:	18-Nov-2020
Complete List of Authors:	<p>Rollinson, Christine; Morton Arboretum, Center for Tree Science Dawson, Andria; Mount Royal University, Department of General Education Raiho, Ann; University of Notre Dame, Department of Biological Sciences Williams, John; University of Wisconsin, Geography; University of Wisconsin-Madison, Center for Climatic Research Dietze, Michael; Boston University, Earth and Environment Hickler, Thomas; Senckenberg Research Institutes and Natural History Museum, Biodiversity and Climate Research Centre; Goethe University Frankfurt, Department of Physical Geography Jackson, Stephen; DOI Southwest Climate Science Center, U.S. Geological Survey; University of Arizona, Dept. of Geosciences McLachlan, Jason; University of Notre Dame, Biological Sciences Moore, David; University of Arizona, School of Natural Resources and the Environment Poulter, Ben; NASA Goddard Space Flight Center, Quaife, Tristan; University of Reading, Department of Meteorology Steinkamp, Jörg; Senckenberg Society for Nature Research, Senckenberg Biodiversity and Climate Research Centre (SBIK-F); Johannes Gutenberg University Trachsel, Mathias; University of Wisconsin-Madison, Department of Geography</p>

1
2
3 **1 Forest responses to last-millennium hydroclimate variability are governed by spatial variations in**
4 **2 ecosystem sensitivity**
5
6

7 **4 Authors:**

- 8 **1. Christine R. Rollinson***, crollinson@mortonarb.org
9 a. Center for Tree Science, The Morton Arboretum, 4100 Illinois Route 53, Lisle,
10 IL, 60532
11 **2. Andria Dawson**, andria.dawson@gmail.com
12 a. Department of General Education, Mount Royal University, Calgary, Alberta,
13 T3E 6K6, Canada
14 **3. Ann M. Raiho**, ann.raiho@gmail.com
15 a. Department of Biological Sciences, University of Notre Dame, 100 Galvin Life
16 Science Center, Notre Dame, IN, 46556,
17 **4. John W. Williams**, jwwilliams1@wisc.edu, jww@geography.wisc.edu
18 a. Department of Geography and Center for Climatic Research, University of
19 Wisconsin-Madison, Madison, WI 53704
20 **5. Michael C. Dietze**, dietze@bu.edu orcid:0000-0002-2324-2518
21 a. Department of Earth and Environment, Boston University, 685 Commonwealth
22 Ave, Boston, MA 02215
23 **6. Thomas Hickler**, thomas.hickler@senckenberg.de
24 a. Senckenberg Biodiversity and Climate Research Centre (SBiK-F),
25 Senckenberganlage 25, 60325 Frankfurt/Main, Germany
26 b. Department of Physical Geography, Goethe University, Frankfurt/Main, Germany
27 **7. Stephen T. Jackson**, jackson@uwyo.edu; stjackson@usgs.gov
28 a. US Geological Survey, Southwest and South Central Climate Adaptation Centers
29 b. Department of Geosciences, University of Arizona, Tucson, AZ 85721
30 **8. Jason McLachlan**, Jason.S.McLachlan.2@nd.edu, jmclachl@nd.edu
31 a. Department of Biological Sciences, University of Notre Dame, 100 Galvin Life
32 Science Center, Notre Dame, IN, 46556
33 **9. David JP Moore**, davidjpmoore@email.arizona.edu
34 a. School of Natural Resources, University of Arizona, Tucson, AZ, 85721
35 **10. Benjamin Poulter**, benjamin.poulter@nasa.gov
36 a. NASA GSFC, Biospheric Sciences Lab., Greenbelt, MD 20771
37 **11. Tristan Quaife**, t.l.quaife@reading.ac.uk
38 a. Department of Meteorology, University of Reading, Reading, RG6 6BB UK
39 **12. Jörg Steinkamp**, steinkamp.joerg@gmail.com
40 a. Senckenberg Biodiversity and Climate Research Centre (SBiK-F),
41 Frankfurt/Main, Germany
42 b. Johannes Gutenberg University, Mainz, Germany
43 **13. Mathias Trachsel**, mtrachs@gmail.com
44 a. Department of Geography, University of Wisconsin-Madison, Madison, WI
45 53704
46
47
48
49
50
51
52
53
54
55
56
57
58
59
60

Running Title

Past forest variability and sensitivity

Keywords

stability, vulnerability, drought, ecosystem modeling, paleoecology, climate change,

Statement of Authorship:

CRR, AD, AMR, and JWW designed the study. AD, AMR, JWW, STJ, JM, and MT created pollen reconstructions and aided in interpretation (STEPPS, ReFAB). AD and AMR wrote the pollen methods. CRR, AMR, MCD, JM, DJPM, BP, TQ, and JS performed ecosystem model simulations and aided in interpretation. CRR and JWW wrote the manuscript with additional input from AD, AMR, and all authors.

Data Accessibility Statement:

Should the manuscript be accepted, the data supporting the results will be archived in two public repositories and the DOIs will be included at the end of this article. Pollen data is already available or will be made available upon acceptance on the EDI data portal as an msb-paleon product. The [Environmental Data Initiative](#) is an NSF-funded program tailored towards environmental data and works closely with the US Long-Term Ecological Research (LTER) Network, NSF Macrosystems Biology program (which funded our work), and DataONE. Terrestrial ecosystem model drivers are being archived on the ORNL DAAC and will be available at the following DOI:

<https://doi.org/10.3334/ORN LDAAC/1779>. The [Oak Ridge National Laboratory Distributed Active Archive Center \(ORNL DAAC\)](#) is managed by NASA's Earth Science Data and Information Systems program and is well suited to archive ecosystem model output, which is often large and has converged on netcdf as a standard file format. These repositories have been approved by *Ecology Letters* editorial staff. All code for analyses is publicly available on Github: <https://github.com/PaleEON-Project/EcosystemVariability>

Manuscript Metadata:**Abstract Word Count:** 147**Manuscript Word Count:** 4,991**Text Box Word Count:** N/A**Number of References:** 67**Number of Figures:** 4**Number of Tables:** 1**Number of Text Boxes:** 0

Corresponding Author: Christine R. Rollinson, Center for Tree Science, The Morton Arboretum, 4100 Illinois Route 53, Lisle, IL 60532; phone: 630-719-2422; email: crollinson@mortonarb.org

1
2
3 **83 Abstract**
4

5 84 Forecasts of future forest change are governed by ecosystem sensitivity to climate change, but
6
7 85 ecosystem model projections are under-constrained by data at multidecadal and longer
8
9 86 timescales. Here, we quantify ecosystem sensitivity to centennial-scale hydroclimate variability,
10
11 87 by comparing dendroclimatic and pollen-inferred reconstructions of drought, forest composition
12
13 88 and biomass for the last millennium with five ecosystem model simulations. In both
14
15 89 observations and models, spatial patterns in ecosystem responses to hydroclimate variability are
16
17 90 strongly governed by ecosystem sensitivity rather than climate exposure. Ecosystem sensitivity
18
19 91 was higher in models than observations and highest in simpler models. Model-data comparisons
20
21 92 suggest that interactions among biodiversity, demography, and ecophysiology processes dampen
22
23 93 the sensitivity of forest composition and biomass to climate variability and change. Integrating
24
25 94 ecosystem models with observations from timescales extending beyond the instrumental record
26
27 95 can better understand and forecast the mechanisms regulating forest sensitivity to climate
28
29 96 variability in a complex and changing world.
30
31
32
33
34

35 97
36
37
38
39
40
41
42
43
44
45
46
47
48
49
50
51
52
53
54
55
56
57
58
59
60

98 Introduction

99 Exposure to 21st-century climate change is expected to profoundly impact global forest
100 composition, diversity, and structure (Dawson *et al.* 2011; Keeley *et al.* 2019), but the sensitivity
101 of ecosystems to climate variability at multi-decadal to centennial time scales is poorly
102 constrained by instrumental observations. Multiple observational studies that employ
103 subcontinental- to continental-scale data networks across a broad range of timescales have
104 sought to empirically estimate the sensitivity of forest ecosystems to climate variability. The
105 sensitivity of tree growth rates, biomass accumulation, and ecophysiological processes to
106 interannual climate variability is well-documented by dendroecological data, with compelling
107 evidence that forest sensitivity to climate depends on forest age and is non-stationary across
108 space and time (Charney *et al.* 2016; Klesse *et al.* 2018; Thom *et al.* 2019; Peltier & Ogle
109 2020). On glacial-interglacial timescales, networks of fossil pollen records show that
110 temperature variations are the primary driver of forest composition and species distributions
111 (Shuman *et al.* 2004; Nolan *et al.* 2018), while over the last several thousand years, hydroclimate
112 variability has strongly affected forest composition and structure in temperate forests of the
113 northeastern and upper midwestern United States (Booth *et al.* 2012; Shuman *et al.* 2019).

114 Terrestrial ecosystem models used to forecast responses to climate change often have
115 difficulty reproducing broad-scale and long-term responses to environmental variability, despite
116 being well-grounded in empirical evidence and ecological theory (Friedlingstein *et al.* 2006,
117 2014; Matthes *et al.* 2016). These models mechanistically connect ecophysiological processes
118 and climate variability to past and present changes in forest composition and structure but are
119 subject to uncertainty in external forcings (e.g., drivers), process representation, and
120 parametrization that complicates data-model comparisons (Figure 1) (LeBauer *et al.* 2013;
121 Matthes *et al.* 2016; Dietze 2017; McLachlan & PaleON Project 2018). Each model includes

1
2
3 122 hypotheses about the primary processes and ecosystem characteristics governing forest change,
4
5 123 various simplifying assumptions, and tradeoffs between computational tractability and process
6
7 124 complexity (De Kauwe *et al.* 2013; Walker *et al.* 2014; Medlyn *et al.* 2015). Previous data-
8
9 125 model comparisons have returned mixed evidence about whether models underestimate or
10
11 126 overestimate the sensitivity of forest processes such as net primary productivity (NPP) and
12
13 127 mortality to climate change (Schimel *et al.* 2015; Walker *et al.* 2015; Rollinson *et al.* 2017). As
14
15 128 a result, projections of forest compositional and structural responses to climate change have high
16
17 129 uncertainty, which propagates to increased uncertainty in science-based adaptation planning
18
19
20 130 (Friedlingstein *et al.* 2014).

21
22
23
24 131 Several challenges have traditionally hindered the joint analysis and integration of
25
26 132 terrestrial ecosystem models and paleoecological data to better constrain modeled responses to
27
28 133 climate variations at multi-decadal and longer timescales. First, the raw observations collected
29
30 134 from fossil pollen records (counts of individual pollen taxa) have no direct counterparts in
31
32 135 ecosystem models. Bayesian hierarchical models are providing new process-based approaches to
33
34 136 infer emergent ecosystem properties from fossil pollen records, such as forest composition,
35
36 137 diversity, percent cover, and biomass (Raiho *et al.* in prep; Blarquez & Aleman 2016; Dawson *et*
37
38 138 *al.* 2016), but the number of state variables that can be estimated from paleoecological data
39
40 139 remains small relative to the number of latent (i.e., unobservable) variables simulated by
41
42 140 ecosystem models (Fig. 1). Second, pre-instrumental model-data comparisons are complicated
43
44 141 by reliance on driver datasets derived from general circulation models (GCMs). GCMs generally
45
46 142 capture macroscale spatial patterns and low-frequency trends in climate but are unable to fully
47
48 143 capture the complexity and stochasticity of local to regional-scale weather phenomena at the
49
50
51 144 subdaily resolution needed to drive ecosystem models, resulting in systematic spatial and
52
53
54
55
56
57
58
59
60

1
2
3 145 temporal biases in model simulations (Anav *et al.* 2013; Matthes *et al.* 2016; Dietze *et al.* 2018).
4
5 146 Third, the native temporal resolution varies between paleodata and models and requires a
6
7 147 temporal standardization. Due to these challenges, the predicted sensitivity of ecosystem model
8
9 148 state variables such as forest composition and biomass to climate change is largely unvalidated
10
11 149 by observations at multidecadal and longer timescales, resulting in wide divergence among
12
13 150 terrestrial ecosystem models in their 21st-century projections (Friedlingstein *et al.* 2006,
14
15 151 2014). Fourth, terrestrial ecosystem models vary widely in represented processes, which can
16
17 152 challenge intermodel comparisons but also provide insight into key governing ecological
18
19 153 processes when data-model discrepancies emerge.
20
21
22
23

24 154 Here, we seek to establish the patterns of forest ecosystem and climate variability in the
25
26 155 north-central and northeastern US for the last millennium (850-1850 C.E.) and identify the
27
28 156 mechanisms underpinning both forest ecosystem sensitivity and observed data-model
29
30 157 discrepancies. In these analyses, we test hypotheses about the relative importance of
31
32 158 hydroclimate exposure, defined as the magnitude of drought variability, and ecosystem
33
34 159 sensitivity as determinants of the variability seen in forest ecosystems. We also hypothesize that
35
36 160 ecosystem models will be overly sensitive to hydroclimate variability due to insufficient
37
38 161 representation of ecophysiological and demographic processes that can dampen climate
39
40 162 responses. To this end, we present a novel series of data-model and model-model comparisons
41
42 163 that are designed to overcome traditional barriers to data-model intercomparison for pre-
43
44 164 instrumental times. Our analyses combine dendroclimatic indices of drought, recently published
45
46 165 Bayesian spatiotemporal estimates of forest composition and biomass derived from pollen that
47
48 166 provide independent checks on last-millennium simulations from five terrestrial ecosystem
49
50 167 models for the northeastern and upper midwestern United States. The data-model comparisons
51
52
53
54
55
56
57
58
59
60

1
2
3 168 discriminate among differing representations of forest processes such as productivity and
4
5 169 demography, while the model-model comparisons help diagnose causal relationships among
6
7
8 170 ecological processes, changes in forest states, and climate variability (Fig. 1). To test hypotheses
9
10 171 while also overcoming known geographic biases in the model simulations of ecosystem state
11
12 172 such as forest composition that source back to biases in the climate model drivers (Matthes *et al.*
13
14 173 2016), we develop a new variability metric that we apply to the data and model-derived products
15
16
17 174 that focuses on comparisons among variability of hydroclimate, composition, and biomass (Fig.
18
19 175 1). Our results indicate that at centennial timescales, spatial patterns in the variability of forest
20
21 176 composition and biomass are regulated by ecological factors such as ecotonal position and
22
23 177 complexity rather than climate exposure as defined by the local magnitude of climate variability.
24
25
26 178

27 28 179 **Materials & Methods**

29 30 180 *Overview*

31
32 181 We employ a combination of data-model and model-model comparisons (Fig. 1) in which
33
34 182 we combine paleoclimatic and paleoecological datasets to draw inferences about past variations
35
36 183 in hydroclimate and forest composition and biomass. The temporal domain of this study is 850-
37
38 184 1850 AD and is bounded by the temporal extent of the climate drivers available for our model
39
40 185 simulations (850 AD) and time of EuroAmerican settlement-era tree surveys (ca. 1850 AD). In
41
42 186 our study, 'data' refers to observation-based statistical models of past drought, forest
43
44 187 composition, and biomass, reconstructed from tree rings, historical tree surveys, and networks of
45
46 188 fossil pollen records. These data-based inferences are fully independent of the ecosystem model
47
48 189 simulations. Model-based comparisons are from the PaleON Ecosystem Model Intercomparison
49
50 190 Project (PEMIP) (Rollinson *et al.* 2017), which used spatially and temporally downscaled past
51
52 191 climate simulations from the Fifth Coupled Model Intercomparison Project (CMIP5) as drivers.
53
54
55
56
57
58
59
60

1
2
3 192 Comparisons among ecosystem model simulations and empirical data rely on normalized values
4
5 193 compared in environmental space, rather than geographic space, in order to reduce the effects of
6
7
8 194 any bias in the climate drivers in our analyses and to focus on sensitivity of ecosystems to
9
10 195 climate variability (Supplemental Figure 1).

11
12 19613
14 197 *Observational Datasets*

15
16 198 The empirically inferred datasets leverage recent advances in pollen-vegetation modeling
17
18 199 (Dawson *et al.* 2016), a form of proxy system modeling (Evans *et al.* 2013) in which ecosystem
19
20 200 state variables such as composition and biomass are estimated along with associated
21
22 201 observational uncertainties. Of the three inferred datasets used here, two were derived from
23
24 202 networks of fossil pollen records provided by individual data contributors and the Neotoma
25
26 203 Paleoecology Database and were calibrated against historical surveys of forest composition and
27
28 204 structure from the early stages of EuroAmerican settlement (Liu *et al.* 2011; Dawson *et al.* 2016;
29
30 205 Goring *et al.* 2016; Kujawa *et al.* 2016; Paciorek *et al.* 2016). Pollen-based inferences are based
31
32 206 on statistical pollen-vegetation models (PVMs) called STEPPS and ReFAB, and represent
33
34 207 fractional vegetation composition and total woody biomass, respectively, for 12 tree genera that
35
36 208 are common elements of upper Midwest forests. STEPPS is a Bayesian hierarchical spatio-
37
38 209 temporal model that infers fractional forest composition from networks of fossil pollen records
39
40 210 (Paciorek & McLachlan 2009; Dawson *et al.* 2016, 2019b; Trachsel *et al.* 2020). STEPPS
41
42 211 employs a process-based representation of pollen dispersal and production, with taxon-specific
43
44 212 parameterizations. STEPPS is calibrated using spatial datasets of pollen samples and forest
45
46 213 composition data, here from the settlement era (Paciorek & McLachlan 2009; Dawson *et al.*
47
48 214 2016), then run for fossil pollen assemblages for other time intervals to produce posterior
49
50 215 estimates of past forest composition. Using this framework, STEPPS: (i) explicitly characterizes
51
52
53
54
55
56
57
58
59
60

1
2
3 216 uncertainty in data and processes, with posterior distributions of process parameters and state
4
5 217 variables such as forest composition, and (ii) borrows information across space and time,
6
7 218 allowing for spatially comprehensive estimates of composition. For both the upper Midwestern
8
9 219 USA (UMW; Minnesota, Wisconsin, Michigan) (Dawson *et al.* 2019a) and the northeastern
10
11 220 USA (NEUS) (Trachsel *et al.* 2020), STEPPS has been used to estimate centennially resolved
12
13 221 forest composition for the late Holocene (250 B.C. to 1750 A.D) at a 24 km grid; here we use the
14
15 222 results from 850 to 1750 AD.
16
17
18

19 223 ReFAB also employs a similar approach to STEPPS but focuses specifically on
20
21 224 estimating total aboveground woody biomass (Raiho *et al.* in prep). ReFAB is calibrated using
22
23 225 the relationship between settlement-era multivariate pollen counts and biomass from PLS
24
25 226 surveys (Paciorek *et al.* 2019). Parameter estimates from calibration are then used to reconstruct
26
27 227 centennially resolved biomass for 77 sites in the UMW for the last 10,000 years (Raiho *et al.* in
28
29 228 prep). ReFAB can characterize the uncertainty in sediment pollen age estimates, calibration
30
31 229 parameters, the relationship between species composition and total aboveground woody biomass,
32
33 230 and species-level allometries.
34
35
36
37

38 231 The Living Blended Drought Atlas (LBDA) provides yearly estimates of summer (mean
39
40 232 June, July, August) Palmer Severity Drought Index (PDSI) for North America, based on
41
42 233 networks of tree-growth chronologies (Cook *et al.* 2010; Woodhouse *et al.* 2010). We used PDSI
43
44 234 as our measure of hydroclimate variability because it is an important predictor of forest dynamics
45
46 235 in this domain and can also be calculated directly from the meteorological forcings used for the
47
48 236 ecosystem model simulations (Clifford & Booth 2015; Cook *et al.* 2015). LBDA PDSIs are
49
50 237 provided at 0.5-degree spatial grid resolution. Due to varying temporal extent of tree-growth
51
52
53
54
55
56
57
58
59
60

1
2
3 238 chronologies, the temporal extent of the LBDA varies. The earliest years in this spatial domain
4
5 239 ranged from 0 to 1671 AD, while the latest year was 2005 (Supplemental Figure 1).
6
7

8 240

9
10 241 *Modeling Datasets*

11
12 242 PEMIP model simulations here are composed of five ecosystem models with dynamic
13
14 243 vegetation (ED2; LINKAGES; LPG-WSL; LPJ-GUESS; and JULES-TRIFFID) run at 254
15
16 244 locations across the eastern and midwestern US at 0.5-degree spatial resolution (Rollinson *et al.*
17
18 245 2020). These models vary in how they characterize forest composition and carbon dynamics and
19
20 246 range from species-based with little ecophysiological process representation (e.g., LINKAGES)
21
22 247 to detailed ecophysiology and cohort representation, but reliance on plant functional types
23
24 248 (PFTs; e.g. ED2, Table 1). LPJ-GUESS and LPJ-WSL both included stochastic fire disturbances
25
26 249 in their simulations, while other models such as ED and LINKAGES include processes of tree
27
28 250 mortality that assume landscape-scale equilibrium (Rollinson *et al.* 2017).
29
30
31

32
33 251 PEMIP climate drivers were temporally downscaled and bias-corrected from existing past
34
35 252 climate simulations to meet the external forcing needs of the ecosystem model ensemble
36
37 253 (Supplemental Figure 1) (Kumar *et al.* 2012; Rollinson *et al.* 2017). CCSM4 output from the
38
39 254 Paleoclimate Modeling Intercomparison Project, Phase III (PMIP3) past millennium simulations
40
41 255 and the Coupled Model Intercomparison Project, Phase 5 (CMIP5) historical simulations were
42
43 256 downscaled to 0.5-degree spatial resolution and 6-hourly temporal resolution using standard
44
45 257 protocols (Kumar *et al.* 2012; Rollinson *et al.* 2017). After the 6-hourly PEMIP climate driver
46
47 258 datasets were created, they were then temporally averaged to meet the specific driver
48
49 259 requirements of individual ecosystem models, which vary in temporal resolution. ED2 and
50
51 260 JULES-TRIFFID use the full suite of 6-hourly drivers for temperature, precipitation, shortwave
52
53
54 261 radiation, longwave radiation, surface pressure, specific humidity, wind speed, and carbon
55
56
57
58
59
60

1
2
3 262 dioxide concentration. Meteorological drivers for the two LPJ variants include daily
4
5 263 temperature, precipitation, and shortwave radiation plus longwave radiation for LPJ-WSL.
6
7
8 264 LINKAGES only requires monthly average temperature and precipitation. Soil texture used to
9
10 265 parameterize locations in model simulations was extracted from the Harmonized World Soil
11
12 266 Database (Wei *et al.* 2014). Monthly temperature and precipitation were combined with soil
13
14 267 water holding capacity computed from model driver soil texture and depth to calculate PDSI,
15
16
17 268 following (Cook *et al.* 2015), but using the Thornthwaite equation for evapotranspiration
18
19 269 (Thornthwaite & Mather 1957; Pelton *et al.* 1960). We used the Thornthwaite equation so that
20
21 270 the calculation of PDSI was independent of internal model dynamics, including
22
23
24 271 evapotranspiration, which can vary widely among ecosystem models, even when given the same
25
26 272 temperature and precipitation drivers, due to differences in model structure and parameterization.
27
28 273 From the ecosystem models, we extracted fractional forest composition and total aboveground
29
30 274 biomass, which can be directly compared to paleoecological observations, and four variables that
31
32 275 are latent, i.e., unobservable in the paleoecological record (Fig. 1): gross primary productivity
33
34 276 (GPP), net primary productivity (NPP), net ecosystem exchange (NEE), and leaf area index
35
36 277 (LAI).
37
38
39
40 278

41 42 279 *Analyses*

43
44 280 Analyses focused on the comparison of empirical data and ecosystem model outputs of
45
46 281 centennial-scale variability in forest composition and biomass driven by drought variability over
47
48 282 the last 1,000 years. Our analytical approach involved three key stages to maximize
49
50 283 commensurability between observations and model output: 1) temporal homogenization of all
51
52 284 variables to a common centennial resolution; 2) development of a common normalized
53
54
55 285 variability metric for ecosystem and drought variability to facilitate comparison across different
56
57
58
59
60

286 variables, and 3) use of hydroclimate sensitivity as the basis for all model-data and model-model
 287 comparisons to minimize the potential effects of biases in the climate model drivers.

288

289 *i. Temporal Homogenization*

290 For annually resolved datasets in our study, including the LBDA and all model output
 291 and drivers, a generalized additive model (GAM) was used to generate time series with the
 292 similar centennial-scale smoothing as the pollen inferred observational datasets. In this process,
 293 the response variable for analysis (e.g. drought, biomass, GPP) was modeled as a function of
 294 time (year) using a thin-plate regression spline with one knot per 100 years (e.g. 10 knots for a
 295 1,000 year window) using the *gam* function in the *mgcv* package in R (Wood 2017; Simpson
 296 2018). To capture the temporal uncertainty similar to that generated in the PVMs, we generated
 297 a 1000-member posterior distribution of each predicted variable through time using the error and
 298 covariance of the intercept and spline parameters. We then extracted the predicted values at 100-
 299 year intervals corresponding to the windows captured by the STEPPS and ReFAB output.

300

301 *ii. Variability Metric*

302 To facilitate comparisons among variables with different units such as composition and
 303 biomass, we developed a base metric for all analyses, consisting of the normalized mean
 304 temporal variability of each dataset (eq. 1).

305 **equation 1:** $variability_i = \ln \frac{\bar{d}_i}{\bar{x}}$

306 **equation 2:** $d_{i,t} = |x_{i,t} - x_{i,t-1}|$

307 Mean temporal variability at each location (\bar{d}_i) for each variable (e.g., composition, biomass,
 308 PDSI) was calculated as the mean of the absolute first differences between adjacent time points

1
2
3 309 $(t, t - 1)$ extracted from centennially resolved time series for each location (i) (eq. 2). The use
4
5 310 of first differences is a discretization of the first derivative and describes the rate of change at
6
7 311 each timestep. Each first-difference calculation was based on the mean of the posterior draws
8
9 312 from the STEPPS or ReFAB PVM or to the GAMs fitted to the LBDA data and ecosystem
10
11 313 model variables. We normalized variability by dividing the mean first differences for each
12
13 314 location (\overline{d}_i) by the variable mean for that dataset across the entire spatiotemporal domain (\overline{x}).
14
15 315 For forest compositional data, the variability metric was calculated using the taxon or plant
16
17 316 functional type (PFT) with the highest fractional composition at each location, with the choice of
18
19 317 taxon or PFT allowed to vary among sites. For all analyses and presented results, normalized
20
21 318 variability is log-transformed to meet standard statistical assumptions of Gaussian distributions
22
23 319 and homoscedasticity (eq. 1).
24
25
26
27
28
29
30

31 321 *iii. Hydroclimate Sensitivity*

32
33 322 After the normalized temporal variability was calculated for PDSI and all ecosystem
34
35 323 variables, sensitivity to hydroclimate variability was defined as the slope of a linear regression
36
37 324 between variability as the independent variable and variability of the ecosystem response
38
39 325 variable such as composition or biomass. These analyses always used the appropriate
40
41 326 observational or modeled PDSI variability (i.e., LBDA for the pollen-inferred compositional
42
43 327 variability; calculated PEMIP driver PDSI variability for the model-simulated compositional
44
45 328 variability) to ensure internal consistency between climatic forcing and ecosystem response.
46
47
48
49
50

51 330 **Results**

52
53 331 In the observational data, variability in forest composition or biomass in the northeastern
54
55 332 US (NEUS) and upper midwestern US (UMW), did not correlate to drought variability (Table 1,
56
57
58
59
60

1
2
3 333 Figs. 2, 3) in contrast with the hypothesis that high exposure to climate variability should lead to
4
5 334 increased compositional variability. Neither the full spatiotemporal domain (Table 1) nor the
6
7 335 UMW (Fig. 3, sensitivity slope = 0.010 SE 0.018) showed a significant relationship between
8
9 336 reconstructed drought and composition variability, although the NEUS showed weak sensitivity
10
11 337 (Fig. 3, sensitivity slope = 0.065 SE 0.027). Reconstructed biomass variability (Fig 2., biomass
12
13 338 reconstructions not available for the NEUS, (Paciorek *et al.* 2019)) also was uncorrelated to
14
15 339 drought variability (Table 1) and instead showed the highest variability at the historic prairie-
16
17 340 forest ecotone (Fig. 2) (Goring & Williams 2017). In pollen-based reconstructions, composition
18
19 341 and biomass variability were weakly but positively related (Fig. 3c, $R^2=0.09$, slope=0.479 SE
20
21 342 0.187) and locations with higher taxonomic richness tended to have higher variability
22
23 343 (Supplemental Fig. 2).

24
25
26 344 Modeled ecosystem sensitivity to drought variability was generally similar to or higher
27
28 345 than observations, with less-complex models tending to have a too-high predicted sensitivity
29
30 346 relative to the empirical reconstructions (Fig. 3). Composition variability was more sensitive to
31
32 347 drought variability than in reconstructions for three of five ecosystem models (ED2, LPJ-WSL,
33
34 348 and TRIFFID), with the data-model discrepancy most pronounced in models with fewer plant
35
36 349 types or taxa (Fig. 3a, Table 1). JULES-TRIFFID, which had only two tree PFTs (deciduous and
37
38 350 evergreen), had the highest drought sensitivity (composition slope = -8.633 SE = 1.075,
39
40 351 composition sensitivity slope 0.411 SE = 0.022). LPJ-WSL and ED2, with respectively six and
41
42 352 five PFTs, had similar mean compositional variability (LPJ-WSL slope = -7.829 SE = 0.943,
43
44 353 ED2 slope = -7.156 SE = 0.514), although LPJ-WSL was approximately twice as sensitive to
45
46 354 hydroclimate variability as ED2 (Fig. 3a, Table 1, LPJ-WSL slope = 0.252 SE =0.018, ED2
47
48 slope = 0.118 SE = 0.018). LINKAGES, which simulated 15 individual species, had among the
49
50
51
52
53
54
55
56
57
58
59
60

1
2
3 356 lowest sensitivity to drought variability (Fig. 3a, Table 1, composition slope = -6.598 SE =
4
5 357 0.478, composition sensitivity slope 0.074 SE = 0.018).

6
7
8 358 Ecosystem models with simpler representation of vegetation ecophysiology
9
10 359 (LINKAGES, JULES-TRIFFID) also had a too-high sensitivity of biomass to drought variability
11
12 360 relative to empirical reconstructions (Table 1, Fig. 3b). Both LINKAGES and JULES-TRIFFID
13
14 361 showed a tight positive coupling of biomass sensitivity to drought variability, which
15
16
17 362 corresponded to strong correlations between biomass and composition variability (Fig. 3c).
18
19 363 LINKAGES showed a one-to-one relationship between composition and biomass variability,
20
21 364 which is much stronger than reconstructions (Fig. 3c). Of all the models, only LPJ-WSL was
22
23 365 consistent with the data in showing a weakly negative relationship between biomass and PDSI
24
25 366 variability (Fig. 3b) while also showing a positive correlation between biomass and composition
26
27 367 variability (Fig. 3c).

28
29
30
31 368 Further analysis of latent variables in the ecosystem models confirmed that variations in
32
33 369 modeled ecosystem sensitivity to hydroclimate variability is linked to model complexity of
34
35 370 ecosystem composition and processes (Fig. 4). There is a cascading series of linkages in
36
37 371 physiological variables within and among taxa (Figs. 1, 4), in which gross primary productivity
38
39 372 (GPP) is directly influenced by temperature and moisture availability, while other state variables
40
41 373 such as net primary productivity (NPP), leaf area index (LAI), and aboveground biomass (AGB)
42
43 374 are regulated by additional downstream processes that may decouple their variability from
44
45 375 climate variability (Fig. 1). Hence, in most models, GPP variability is the most sensitive to
46
47 376 drought variability (Fig. 4, Supplemental Table 1). In all models, sensitivity of forest
48
49 377 composition to drought variability seems to be most closely linked to sensitivity of NPP. NPP
50
51 378 sensitivity tended to be higher in low-diversity models such as JULES-TRIFFID (Figure 4,
52
53
54
55
56
57
58
59
60

1
2
3 379 Supplemental Table 1). Higher diversity through more tree types or taxa was associated with
4
5 380 higher compositional variability and reduced sensitivity to drought (Figure 3, Table 1,
6
7 381 Supplemental Figure 2).

8
9
10 382 Models with more detailed representation of plant ecophysiology and either demography
11
12 383 or disturbance (e.g., ED2, LPJ-GUESS, LPJ-WSL) also tended to have lower biomass sensitivity
13
14 384 to hydroclimate variability (Fig. 4) and agree more closely with observations (Fig. 3). Biomass
15
16 385 sensitivity to drought variability in our model ensemble was similar to NEE sensitivity in all
17
18 386 models except LPJ-GUESS (Fig. 4, Supplemental Table 1). LINKAGES and JULES-TRIFFID
19
20 387 may be overly sensitive to hydroclimate variability for entirely different reasons. LINKAGES
21
22 388 has a fairly simple representation of ecophysiological processes while being able to represent
23
24 389 species-level demographic dynamics (Table 1). In contrast, JULES-TRIFFID contains a
25
26 390 sophisticated representation of ecophysiology but for only two tree PFTs and five PFTs total
27
28 391 (Table 1). The other models tend to be more intermediate cases, with intermediate to more
29
30 392 sophisticated representations of both ecophysiology and vegetation dynamics.
31
32
33
34
35
36
37
38
39
40
41
42
43
44
45
46
47
48
49
50
51
52
53
54
55
56
57
58
59
60

394 Discussion

395 Over the last millennium (850-1850 A.D.), both paleodata networks and model
396 simulations suggest that spatial patterns in forest composition and biomass variability in
397 northeastern and upper midwestern United States are governed more by spatial variations in
398 ecosystem sensitivity and less by spatial variations in exposure to climate variability. Ecotonal
399 regions such as the prairie-forest border have higher variability in composition and structure than
400 areas of high PDSI variability (Fig. 2). The intermodel comparisons suggest that added
401 complexity allows slow-to-change variables such as composition and biomass to be insensitive to
402 climate variability at centennial scales despite sensitivity of fast-changing ecophysiological

1
2
3 403 processes such as gross and net primary productivity (Fig. 4). Incorporation of ecological
4
5 404 processes and characteristics such as diversity and demography all tend to reduce simulated
6
7
8 405 climate sensitivity and better align simulations with observations (Figs. 3, 4).
9

10 406 These analyses represent a milestone towards the goal of more comprehensive and
11
12 407 rigorous data-model comparisons for timescales and time periods extending beyond the
13
14 408 instrumental record. Common challenges for multi-centennial data-model comparisons include
15
16
17 409 1) a need for process-informed statistical models of inference for paleoecological data, 2)
18
19 410 generally lower temporal resolution in paleoecological data than in model simulations and with
20
21 411 more latent variables than for the instrumental period, 3) biases in paleoclimatic simulations
22
23 412 leading to biases in ecosystem model simulations, and 4) differences among models in driver
24
25 413 datasets and represented processes. The pollen-vegetation models used in our study include
26
27 414 processes for pollen productivity and dispersal that translates relative pollen abundances into
28
29 415 metrics of forest composition and biomass that can be directly compared to those produced by
30
31 416 ecosystem models (Paciorek & McLachlan 2009; Dawson *et al.* 2016). We further increased the
32
33 417 commensurability between centennially resolved pollen-based quantifications of forest change
34
35 418 and higher-frequency information from tree rings and ecosystem models by using GAMs to
36
37 419 achieve time series with similarly temporally smoothed properties (Simpson 2018). By focusing
38
39 420 on time series variability rather than directly comparing magnitude and timing of change in
40
41 421 specific geographic locations or taxonomic groupings we were able to overcome documented
42
43 422 ecosystem model biases arising from driver, process, and parameter limitations (Matthes *et al.*
44
45 423 2016; Dietze 2017). Finally, we leveraged differences in process representation among models
46
47 424 as a means of evaluating the importance of specific ecosystem processes for producing emergent
48
49
50
51
52
53
54
55
56
57
58
59
60

1
2
3 425 patterns of climate sensitivity that are consistent with paleoecological data (Medlyn *et al.* 2015;
4
5 426 McLachlan & PaleON Project 2018).

7 427 Prior studies have indicated that forest composition and growth is sensitive to climate
8
9 428 variability at annual to centennial scales (Shuman *et al.* 2004; Allen *et al.* 2010; Thom *et al.*
10
11 429 2019), yet there is also increasingly strong evidence that tree-climate relationships are non-
12
13 430 stationary and subject to multiple interacting factors, leading to spatially complex forest
14
15 431 responses to climate change (Girardin *et al.* 2016) and variations in climatic sensitivity across
16
17 432 space and time (Rollinson *et al.* in press; Thom *et al.* 2019; Peltier & Ogle 2020; Wilmking *et al.*
18
19 433 2020). Several possible explanations exist for the reporting here of generally low sensitivity of
20
21 434 forest composition and biomass to hydroclimate in reconstructions (Fig. 2). First, this apparent
22
23 435 insensitivity may be due to the temporal grain of this study. The centennially resolved temporal
24
25 436 grain of our analyses limits detection of annual-scale growth variations, the effects of stochastic
26
27 437 or short-lived extreme events such as sub-decadal to decadal drought (Breshears *et al.* 2005;
28
29 438 Allen *et al.* 2010; Seidl *et al.* 2011), or disturbance events such as fire and pest outbreaks, unless
30
31 439 these are large enough to cause stand-replacing mortality events. Disturbance processes are
32
33 440 often unrepresented in ecosystem models or treated as purely stochastic and with implicit
34
35 441 assumptions of landscape-scale equilibria (Seidl *et al.* 2011; Fisher *et al.* 2018; McCabe &
36
37 442 Dietze 2019). Of the ecosystem models used here, LPJ-WSL and LPJ-GUESS included fire in
38
39 443 their simulations as a semi-mechanistic process following GLOBFIRM (Thonicke *et al.* 2001),
40
41 444 which estimates burned area as a function of daily fire probabilities that are a function of fuel
42
43 445 moisture and fuel load threshold. These models showed dampened biomass sensitivity to
44
45 446 hydroclimate variability that was more closely aligned with observations (Fig. 4), but so did
46
47 447 ED2, which lacked fire. Hence, process representation of fire or similar semi-stochastic
48
49
50
51
52
53
54
55
56
57
58
59
60

1
2
3 448 disturbances is not a clear differentiator among modelled estimates of ecosystem climate
4
5 449 sensitivity.

6
7
8 450 Second, apparent climate sensitivity might increase if the temporal extent was increased
9
10 451 to include larger climate variations during the Holocene and last deglaciation. Although the last
11
12 452 millennium includes climatic events such as the Medieval Climate Anomaly and Little Ice Age
13
14 453 (PAGES 2k Consortium 2013), these climate variations appear to have been muted relative to
15
16 454 earlier hydroclimate and temperature variations (Fischer *et al.* 2018). During the Holocene,
17
18 455 hydroclimatic variability around the North Atlantic appears to have been an important driver of
19
20 456 forest compositional changes and the collapses of individual tree species (Shuman *et al.* 2019).
21
22 457 Large vegetation changes associated with the abrupt temperature variations of the Younger
23
24 458 Dryas and last deglaciation are well documented (Williams *et al.* 2011), but the temporal extent
25
26 459 of this study was constrained by the temporal extent of the last-millennium PMIP3/CMIP5
27
28 460 simulations used to drive ecosystem models (Braconnot *et al.* 2011; Taylor *et al.* 2012). As the
29
30 461 next generation of transient Holocene simulations become available, the conclusions reached
31
32 462 here about low apparent sensitivity can be revisited.

33
34 463 Third, this paper focuses on spatial patterns of climate and ecosystem variability, whereas
35
36 464 most prior paleoecological studies have tended to focus on temporal variations (Shuman *et al.*
37
38 465 2004; Booth *et al.* 2012). Our analyses of low sensitivity are consistent with recent
39
40 466 dendroecological studies of climate-driven rates of tree growth, which are quickly shifting from
41
42 467 assumptions of stationary tree-climate relationships to demonstrations of spatially complex forest
43
44 468 responses (Girardin *et al.* 2016) and variations in climatic sensitivity varies across space and
45
46 469 time (Rollinson *et al.* in press; Thom *et al.* 2019; Peltier & Ogle 2020; Wilmking *et al.* 2020).
47
48 470 By focusing on spatial variations in ecosystem variability over the last millennium, our analyses
49
50
51
52
53
54
55
56
57
58
59
60

1
2
3 471 suggest spatial variation in ecosystem properties are a more important regulator than spatial
4
5 472 variations in climate exposure. Finally, uncertainties in the proxy-based reconstructions may
6
7 473 lower correlations as detrending techniques used to remove non-climatic signals such as age
8
9 474 effects may dampen estimates of centennial-scale variability (Allen *et al.* 2018; Esper *et al.*
10
11 475 2018). Despite lower PDSI variability in the LBDA than model drivers, we do not think that
12
13 476 spatial variability in hydroclimate variability in the empirical dataset is too low to detect effects
14
15 477 on ecosystem variability. For example, hydroclimate data syntheses for the last 2000 years
16
17 478 suggest opposite patterns of hydroclimate variations between Minnesota/Wisconsin and New
18
19 479 England, which explain 30% of variance in the hydroclimate records (Shuman *et al.* 2019).

20
21
22
23
24 480 Process-based ecosystem models are the main vehicle for forecasting climate-driven
25
26 481 ecosystem dynamics across a range of timescales and in principle are better able to accommodate
27
28 482 past and future no-analog climates (Williams & Jackson 2007; Veloz *et al.* 2012). However, all
29
30 483 ecosystem models face tradeoffs in their ability to represent taxonomic or functional diversity
31
32 484 versus detailed ecophysiological processes that drive ecosystem change (Fisher *et al.* 2018).
33
34 485 Process-based ecosystem models will never be able to capture the full complexity of ecosystems
35
36 486 nor perfectly reproduce the patterns of climatological or ecological variability observed in the
37
38 487 past due to observational uncertainties and incomplete constraints of many processes and
39
40 488 parameterizations (Dietze 2017). This paper has shown how multiple paleoecological data
41
42 489 streams can be combined with harmonized paleoclimatic simulations and multiple terrestrial
43
44 490 ecosystem models to gain new insight into a) how diversity and biological processes can dampen
45
46 491 ecosystem sensitivity to drought variability at broad spatial scales and b) the importance of
47
48 492 complex representations of these aspects of ecosystems to achieve better agreement with the
49
50 493 data. Nevertheless, these analyses followed a traditional approach in which past ecosystem
51
52
53
54
55
56
57
58
59
60

1
2
3 494 reconstructions and simulations were run independently and compared at the final stage of
4
5 495 analysis. The next major step forward is to move to a full data-assimilation framework, in which
6
7 496 paleoecological observations and simulations are combined to overcome systematic biases in
8
9 497 model drivers, parameterization, and output to better evaluate paleoecological change using
10
11 498 mechanistic process-based frameworks (McLachlan & PaleON Project 2018). Through this
12
13 499 iterative process that draws upon an ever-growing and diversifying suite of observational data
14
15 500 streams (Farley *et al.* 2018), we can better understand the mechanisms regulating forest
16
17 501 sensitivity to climate variability across a broad range of timescales and thereby better forecast
18
19 502 future forest dynamics in a complex and rapidly changing world.
20
21
22
23
24
25

26 504 **Acknowledgements**

27
28 505 This work reflects the efforts of the Paleoecological Observatory Network (PaleON Project),
29
30 506 funded by the National Science Foundation MacroSystems Biology under grants DEB-1241891,
31
32 507 DEB-1241868, DEB-1241874, and DEB-1241851 and special thanks to Jody Peters, PaleON
33
34 508 Project coordinator. PDSI calculations from ecosystem model drivers were derived from code
35
36 509 graciously provided by Ben Cook. Fossil pollen data were obtained from the Neotoma
37
38 510 Paleoecology Database (<http://www.neotomadb.org>) and its constituent database the North
39
40 511 American Pollen Database. The work of the data contributors, data stewards, and the Neotoma
41
42 512 community is gratefully acknowledged. Any use of trade, firm, or product names is for
43
44 513 descriptive purposes only and does not imply endorsement by the U.S. Government.
45
46
47
48
49

50 514 **References**

51 516 Allen, C.D., Macalady, A.K., Chenchouni, H., Bachelet, D., McDowell, N., Vennetier, M., *et al.* (2010).
52 517 A global overview of drought and heat-induced tree mortality reveals emerging climate change
53 518 risks for forests. *For. Ecol. Manag.*, 259, 660–684.
54
55
56
57
58
59
60

- 1
2
3 519 Allen, K.J., Villalba, R., Lavergne, A., Palmer, J.G., Cook, E.C., Fenwick, P., *et al.* (2018). A comparison
4 520 of some simple methods used to detect unstable temperature responses in tree-ring chronologies.
5 521 *Dendrochronologia*, 48, 52–73.
- 6 522 Anav, A., Friedlingstein, P., Kidston, M., Bopp, L., Ciais, P., Cox, P., *et al.* (2013). Evaluating the Land
7 523 and Ocean Components of the Global Carbon Cycle in the CMIP5 Earth System Models. *J.*
8 524 *Clim.*, 26, 6801–6843.
- 9 525 Blarquez, O. & Aleman, J.C. (2016). Tree biomass reconstruction shows no lag in postglacial
10 526 afforestation of eastern Canada. *Can. J. For. Res.*, 46, 485–498.
- 11 527 Booth, R.K., Jackson, S.T., Sousa, V.A., Sullivan, M.E., Minckley, T.A. & Clifford, M.J. (2012). Multi-
12 528 decadal drought and amplified moisture variability drove rapid forest community change in a
13 529 humid region. *Ecology*, 93, 219–226.
- 14 530 Braconnot, P., Otto-Bliesner, B., Jungclauss, J. & Peterschmitt, J.-Y. (2011). The Paleoclimate Modeling
15 531 Intercomparison Project contribution to CMIP5. *CLIVAR Exch.*, 16, 15–19.
- 16 532 Breshears, D.D., Cobb, N.S., Rich, P.M., Price, K.P., Allen, C.D., Balice, R.G., *et al.* (2005). Regional
17 533 vegetation die-off in response to global-change-type drought. *Proc. Natl. Acad. Sci.*, 102, 15144–
18 534 15148.
- 19 535 Charney, N.D., Babst, F., Poulter, B., Record, S., Trouet, V.M., Frank, D., *et al.* (2016). Observed forest
20 536 sensitivity to climate implies large changes in 21st century North American forest growth. *Ecol.*
21 537 *Let.*, 19, 1119–1128.
- 22 538 Clifford, M.J. & Booth, R.K. (2015). Late-Holocene drought and fire drove a widespread change in forest
23 539 community composition in eastern North America. *The Holocene*, 25, 1102–1110.
- 24 540 Cook, B.I., Ault, T.R. & Smerdon, J.E. (2015). Unprecedented 21st century drought risk in the American
25 541 Southwest and Central Plains. *Sci. Adv.*, 1, e1400082.
- 26 542 Cook, E.R., Seager, R., Heim, R.R., Vose, R.S., Herweijer, C. & Woodhouse, C. (2010). Megadroughts in
27 543 North America: placing IPCC projections of hydroclimatic change in a long-term palaeoclimate
28 544 context. *J. Quat. Sci.*, 25, 48–61.
- 29 545 Dawson, A., Goring, S., Paciorek, C.J., Jackson, S.T., McLachlan, J.S. & Williams, J.W. (2019a).
30 546 *STEPPS 2000 Year Forest Composition Estimates, Upper Midwest US, Level 2*. Environmental
31 547 Data Initiative.
- 32 548 Dawson, A., Paciorek, C.J., Goring, S.J., Jackson, S.T., McLachlan, J.S. & Williams, J.W. (2019b).
33 549 Quantifying trends and uncertainty in prehistoric forest composition in the upper Midwestern
34 550 United States. *Ecology*, 100.
- 35 551 Dawson, A., Paciorek, C.J., McLachlan, J.S., Goring, S., Williams, J.W. & Jackson, S.T. (2016).
36 552 Quantifying pollen-vegetation relationships to reconstruct ancient forests using 19th-century
37 553 forest composition and pollen data. *Quat. Sci. Rev.*, 137, 156–175.
- 38 554 Dawson, T.P., Jackson, S.T., House, J.I., Prentice, I.C. & Mace, G.M. (2011). Beyond predictions:
39 555 biodiversity conservation in a changing climate. *Science*, 332.
- 40 556 De Kauwe, M.G., Medlyn, B.E., Zaehle, S., Walker, A.P., Dietze, M.C., Hickler, T., *et al.* (2013). Forest
41 557 water use and water use efficiency at elevated CO₂: a model-data intercomparison at two
42 558 contrasting temperate forest FACE sites. *Glob. Change Biol.*, 19, 1759–1779.
- 43 559 Dietze, M.C. (2017). Prediction in ecology: a first-principles framework. *Ecol. Appl.*, 27, 2048–2060.
- 44 560 Dietze, M.C., Fox, A., Beck-Johnson, L.M., Betancourt, J.L., Hooten, M.B., Jarnevich, C.S., *et al.* (2018).
45 561 Iterative near-term ecological forecasting: Needs, opportunities, and challenges. *Proc. Natl. Acad.*
46 562 *Sci.*, 115, 1424–1432.
- 47 563 Esper, J., George, S.St., Anchukaitis, K., D'Arrigo, R., Ljungqvist, F.C., Luterbacher, J., *et al.* (2018).
48 564 Large-scale, millennial-length temperature reconstructions from tree-rings. *Dendrochronologia*,
49 565 50, 81–90.
- 50 566 Evans, M.N., Tolwinski-Ward, S.E., Thompson, D.M. & Anchukaitis, K.J. (2013). Applications of proxy
51 567 system modeling in high resolution paleoclimatology. *Quat. Sci. Rev.*, 76, 16–28.
- 52 568 Farley, S.S., Dawson, A., Goring, S.J. & Williams, J.W. (2018). Situating Ecology as a Big-Data Science:
53 569 Current Advances, Challenges, and Solutions. *BioScience*, 68, 563–576.
- 54
55
56
57
58
59
60

- 1
2
3 570 Fischer, H., Meissner, K.J., Mix, A.C., Abram, N.J., Austermann, J., Brovkin, V., *et al.* (2018).
4 571 Palaeoclimate constraints on the impact of 2 °C anthropogenic warming and beyond. *Nat.*
5 572 *Geosci.*, 11, 474–485.
- 6 573 Fisher, R.A., Koven, C.D., Anderegg, W.R.L., Christoffersen, B.O., Dietze, M.C., Farris, C.E., *et al.*
7 574 (2018). Vegetation demographics in Earth System Models: A review of progress and priorities.
8 575 *Glob. Change Biol.*, 24, 35–54.
- 9 576 Friedlingstein, P., Cox, P., Betts, R., Bopp, L., von Bloh, W., Brovkin, V., *et al.* (2006). Climate–Carbon
10 577 Cycle Feedback Analysis: Results from the C⁴ MIP Model Intercomparison. *J. Clim.*, 19, 3337–
11 578 3353.
- 12 579 Friedlingstein, P., Meinshausen, M., Arora, V.K., Jones, C.D., Anav, A., Liddicoat, S.K., *et al.* (2014).
13 580 Uncertainties in CMIP5 Climate Projections due to Carbon Cycle Feedbacks. *J. Clim.*, 27, 511–
14 581 526.
- 15 582 Girardin, M.P., Bouriaud, O., Hogg, E.H., Kurz, W., Zimmermann, N.E., Metsaranta, J.M., *et al.* (2016).
16 583 No growth stimulation of Canada’s boreal forest under half-century of combined warming and
17 584 CO₂ fertilization. *Proc. Natl. Acad. Sci.*, 113, E8406–E8414.
- 18 585 Goring, S.J., Mladenoff, D.J., Cogbill, C.V., Record, S., Paciorek, C.J., Jackson, S.T., *et al.* (2016). Novel
19 586 and Lost Forests in the Upper Midwestern United States, from New Estimates of Settlement-Era
20 587 Composition, Stem Density, and Biomass. *PLOS ONE*, 11, e0151935.
- 21 588 Keeley, J.E., van Mantgem, P. & Falk, D.A. (2019). Fire, climate and changing forests. *Nat. Plants*, 5,
22 589 774–775.
- 23 590 Klesse, S., Babst, F., Lienert, S., Spahni, R., Joos, F., Bouriaud, O., *et al.* (2018). A Combined Tree Ring
24 591 and Vegetation Model Assessment of European Forest Growth Sensitivity to Interannual Climate
25 592 Variability. *Glob. Biogeochem. Cycles*.
- 26 593 Kujawa, E.R., Goring, S., Dawson, A., Calcote, R., Grimm, E.C., Hotchkiss, S.C., *et al.* (2016). The
27 594 effects of anthropogenic land cover change on pollen-vegetation relationships in the American
28 595 Midwest. *Anthropocene*, 15, 60–71.
- 29 596 Kumar, J., Brooks, B.-G.J., Thornton, P.E. & Dietze, M.C. (2012). Sub-daily Statistical Downscaling of
30 597 Meteorological Variables Using Neural Networks. *Procedia Comput. Sci.*, 9, 887–896.
- 31 598 LeBauer, D.S., Wang, D., Richter, K.T., Davidson, C.C. & Dietze, M.C. (2013). Facilitating feedbacks
32 599 between field measurements and ecosystem models. *Ecol. Monogr.*, 83, 133–154.
- 33 600 Liu, F., Mladenoff, D.J., Keuler, N.S. & Moore, L.S. (2011). Broad-scale variability in tree data of the
34 601 historical Public Land Survey and its consequences for ecological studies. *Ecol. Monogr.*, 81,
35 602 259–275.
- 36 603 Matthes, J.H., Goring, S., Williams, J.W. & Dietze, M.C. (2016). Benchmarking historical CMIP5 plant
37 604 functional types across the Upper Midwest and Northeastern United States. *J. Geophys. Res.*
38 605 *Biogeosciences*, 121, 523–535.
- 39 606 McCabe, T.D. & Dietze, M.C. (2019). Scaling Contagious Disturbance: A Spatially-Implicit Dynamic
40 607 Model. *Front. Ecol. Evol.*, 7.
- 41 608 McLachlan, J.S. & PaleON Project. (2018). Forecasting long-term ecological dynamics using open
42 609 paleodata. *Past Glob. Change Mag.*, 26, 76–76.
- 43 610 Medlyn, B.E., Zaehle, S., De Kauwe, M.G., Walker, A.P., Dietze, M.C., Hanson, P.J., *et al.* (2015). Using
44 611 ecosystem experiments to improve vegetation models. *Nat. Clim. Change*, 5, 528–534.
- 45 612 Nolan, C., Overpeck, J.T., Allen, J.R.M., Anderson, P.M., Betancourt, J.L., Binney, H.A., *et al.* (2018).
46 613 Past and future global transformation of terrestrial ecosystems under climate change. *Science*,
47 614 361, 920–923.
- 48 615 Paciorek, C.J., Cogbill, C.V., Peters, J.A., Goring, S.J., Williams, J.W., Mladenoff, D.J., *et al.* (2019).
49 616 *Statistically-estimated tree biomass, stem density, and basal area for the upper Midwestern*
50 617 *United States at the time of Euro-American settlement* (preprint). Ecology.
- 51 618 Paciorek, C.J., Goring, S.J., Thurman, A.L., Cogbill, C.V., Williams, J.W., Mladenoff, D.J., *et al.* (2016).
52 619 Statistically-Estimated Tree Composition for the Northeastern United States at Euro-American
53 620 Settlement. *PLOS ONE*, 11, e0150087.
- 54
55
56
57
58
59
60

- 1
2
3 621 Paciorek, C.J. & McLachlan, J.S. (2009). Mapping Ancient Forests: Bayesian Inference for Spatio-
4 622 Temporal Trends in Forest Composition Using the Fossil Pollen Proxy Record. *J. Am. Stat.*
5 623 *Assoc.*, 104, 608–622.
- 6 624 PAGES 2k Consortium. (2013). Continental-scale temperature variability during the past two millennia.
7 625 *Nat. Geosci.*, 6, 339–346.
- 8 626 Peltier, D.M.P. & Ogle, K. (2020). Tree growth sensitivity to climate is temporally variable. *Ecol. Lett.*,
9 627 1–20.
- 10 628 Pelton, W.L., King, K.M. & Tanner, C.B. (1960). An evaluation of the Thornthwaite and mean
11 629 temperature methods for determining potential evapotranspiration. *Agron. J.*, 52, 387–395.
- 12 630 Raiho, A.M., Paciorek, C.J. & McLachlan, J.S. (in prep). Species migrations created a 5,000 year regional
13 631 carbon sink past.
- 14 632 Rollinson, C., Dietze, M., Mathes, J.H., Steinkamp, J., Hickler, T., Poulter, B., *et al.* (2020). *PalEON:*
15 633 *Terrestrial Ecosystem Model Ensemble for the Northeastern U.S., 850–2010*. ORNL Distributed
16 634 Active Archive Center.
- 17 635 Rollinson, C.R., Finley, A.O., Alexander, M.R., Banerjee, S., Dixon Hamil, K.-A., Koenig, L., *et al.* (in
18 636 press). Working across space and time: nonstationarity in ecological research and application.
19 637 *Front. Ecol. Environ.*
- 20 638 Rollinson, C.R., Liu, Y., Raiho, A., Moore, D.J.P., McLachlan, J., Bishop, D.A., *et al.* (2017). Emergent
21 639 climate and CO₂ sensitivities of net primary productivity in ecosystem models do not agree with
22 640 empirical data in temperate forests of eastern North America. *Glob. Change Biol.*, 23, 2755–
23 641 2767.
- 24 642 Schimel, D., Stephens, B.B. & Fisher, J.B. (2015). Effect of increasing CO₂ on the terrestrial carbon
25 643 cycle. *Proc. Natl. Acad. Sci.*, 112, 436–441.
- 26 644 Seidl, R., Fernandes, P.M., Fonseca, T.F., Gillet, F., Jönsson, A.M., Merganičová, K., *et al.* (2011).
27 645 Modelling natural disturbances in forest ecosystems: a review. *Ecol. Model.*, 222, 903–924.
- 28 646 Shuman, B., Newby, P., Huang, Y. & Webb, T. (2004). Evidence for the close climatic control of New
29 647 England vegetation history. *Ecology*, 85, 1297–1310.
- 30 648 Shuman, B.N., Marsicek, J., Oswald, W.W. & Foster, D.R. (2019). Predictable hydrological and
31 649 ecological responses to Holocene North Atlantic variability. *Proc. Natl. Acad. Sci.*, 116, 5985–
32 650 5990.
- 33 651 Simpson, G.L. (2018). Modelling Palaeoecological Time Series Using Generalised Additive Models.
34 652 *Front. Ecol. Evol.*, 6.
- 35 653 Taylor, K.E., Stouffer, R.J. & Meehl, G.A. (2012). An Overview of CMIP5 and the Experiment Design.
36 654 *Bull. Am. Meteorol. Soc.*, 93, 485–498.
- 37 655 Thom, D., Golivets, M., Edling, L., Meigs, G.W., Gourevitch, J.D., Sonter, L.J., *et al.* (2019). The climate
38 656 sensitivity of carbon, timber, and species richness covaries with forest age in boreal–temperate
39 657 North America. *Glob. Change Biol.*, 25, 1446–2458.
- 40 658 Thonicke, K., Venevsky, S., Sitch, S. & Cramer, W. (2001). The role of fire disturbance for global
41 659 vegetation dynamics: coupling fire into a Dynamic Global Vegetation Model. *Glob. Ecol.*
42 660 *Biogeogr.*, 10, 661–677.
- 43 661 Thornthwaite, C.W. & Mather, J.R. (1957). Instructions and tables for computing potential
44 662 evapotranspiration and the water balance. *Publ. Climatol.*, 10, 185–311.
- 45 663 Trachsel, M., Dawson, A., Paciorek, C.J., Williams, J.W., McLachlan, J.S., Cogbill, C.V., *et al.* (2020).
46 664 Comparison of settlement-era vegetation reconstructions for STEPPS and REVEALS pollen–
47 665 vegetation models in the northeastern United States. *Quat. Res.*, 95, 23–42.
- 48 666 Veloz, S.D., Williams, J.W., Blois, J.L., He, F., Otto-Bliesner, B. & Liu, Z. (2012). No-analog climates
49 667 and shifting realized niches during the late quaternary: implications for 21st-century predictions
50 668 by species distribution models. *Glob. Change Biol.*, 18, 1698–1713.
- 51 669 Walker, A.P., Hanson, P.J., De Kauwe, M.G., Medlyn, B.E., Zaehle, S., Asao, S., *et al.* (2014).
52 670 Comprehensive ecosystem model-data synthesis using multiple data sets at two temperate forest
53
54
55
56
57
58
59
60

- 1
2
3 671 free-air CO₂ enrichment experiments: Model performance at ambient CO₂ concentration: FACE
4 672 MODEL-DATA SYNTHESIS. *J. Geophys. Res. Biogeosciences*, 119, 937–964.
5 673 Walker, A.P., Zaehle, S., Medlyn, B.E., De Kauwe, M.G., Asao, S., Hickler, T., *et al.* (2015). Predicting
6 674 long-term carbon sequestration in response to CO₂ enrichment: How and why do current
7 675 ecosystem models differ? *Glob. Biogeochem. Cycles*, 29, 476–495.
8 676 Wei, Y., Liu, S., Huntzinger, D.N., Michalak, A.M., Viovy, N., Post, W.M., *et al.* (2014). The North
9 677 American Carbon Program Multi-scale Synthesis and Terrestrial Model Intercomparison Project
10 678 – Part 2: Environmental driver data. *Geosci. Model Dev.*, 7, 2875–2893.
11 679 Williams, J.W., Blois, J.L. & Shuman, B.N. (2011). Extrinsic and intrinsic forcing of abrupt ecological
12 680 change: case studies from the late Quaternary: Extrinsic and intrinsic abrupt ecological change. *J.*
13 681 *Ecol.*, 99, 664–677.
14 682 Williams, J.W. & Jackson, S.T. (2007). Novel Climates, No-Analog Communities, and Ecological
15 683 Surprises. *Front. Ecol. Environ.*, 5, 475–482.
16 684 Wilmking, M., Maaten-Theunissen, M., Maaten, E., Scharnweber, T., Buras, A., Biermann, C., *et al.*
17 685 (2020). Global assessment of relationships between climate and tree growth. *Glob. Change Biol.*,
18 686 26, 3212–3220.
19 687 Wood, S.N. (2017). *Generalized Additive Models: An Introduction with R*. 2nd edn. Chapman and
20 688 Hall/CRC, New York.
21 689 Woodhouse, C.A., Meko, D.M., MacDonald, G.M., Stahle, D.W. & Cook, E.R. (2010). A 1,200-year
22 690 perspective of 21st century drought in southwestern North America. *Proc. Natl. Acad. Sci.*, 107,
23 691 21283–21288.
24 692
25
26
27 693
28
29
30
31
32
33
34
35
36
37
38
39
40
41
42
43
44
45
46
47
48
49
50
51
52
53
54
55
56
57
58
59
60

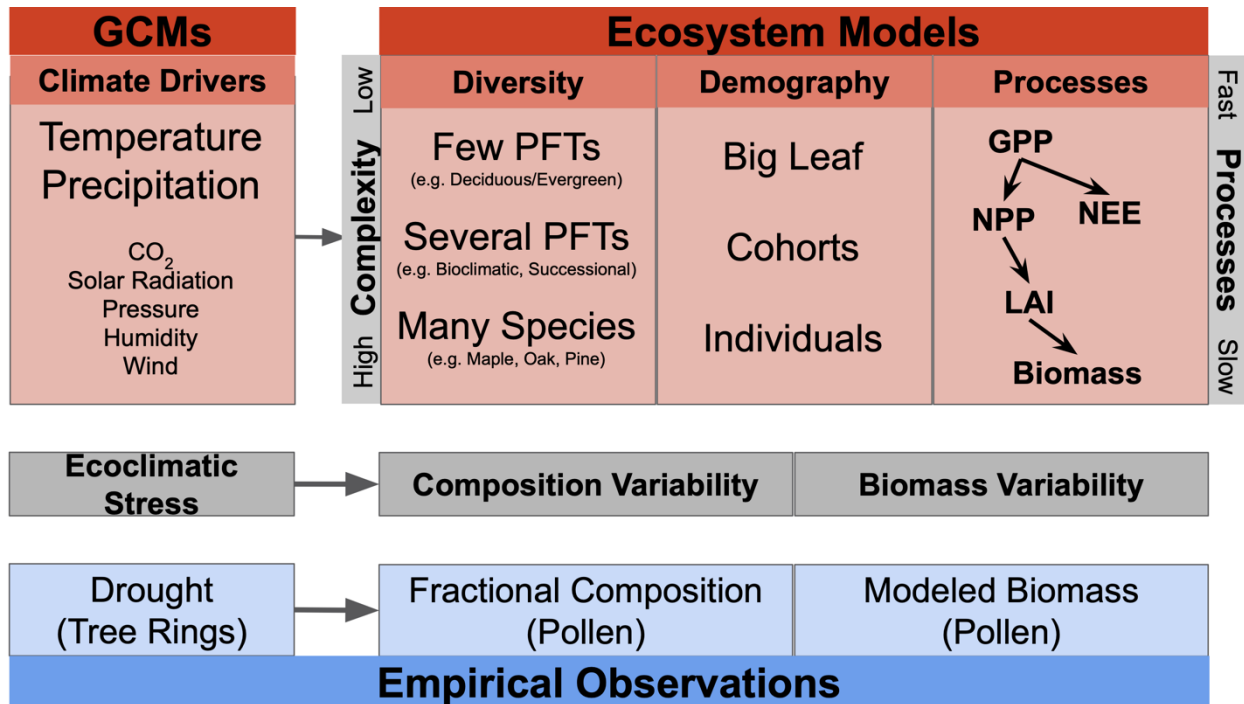
694 **Manuscript Tables**

695 **Table 1:** Comparison of 1) ecosystem model complexity, based on representation of diversity,
 696 demographic, and ecophysiological processes with 2) variability in forest composition (Comp) and
 697 biomass (Biom) and sensitivity to hydroclimate variability. Variability is a normalized metric of total
 698 change in the centennially resolved time series. Sensitivity is presented as the slope and standard error of
 699 linear regression between composition or biomass variability and hydroclimate variability. PFT = plant
 700 functional types. For sensitivity columns, * indicates slopes significantly different from zero ($p < 0.05$); †
 701 indicates model slope significantly different from pollen ($p < 0.05$).

Data Source & Model Name	Tree Diversity Representation	Demographic Representation	Vegetation Processes	Comp. Var. (SD)	Comp. Sens. (SE)	Biom. Var. (SD)	Biom. Sens. (SE)
Pollen: STEPPS, ReFAB	Genera: 12 trees	relative abundance	[implicit]	-2.032 (0.617)	0.026 (0.019)	-7.798 (0.770)	-0.156 (0.119)
ED2	PFTs: 5 tree	cohort	photosynthesis, allocation, cross-PFT competition, cross-cohort competition	-7.156 (0.514)	0.118 (0.018)*†	-7.505 (0.446)	-0.079 (0.027)*
LINK-AGES	Species: 15 tree	individual	cross-PFT competition, cross-cohort competition	-6.598 (0.478)	0.074 (0.018)*	-6.741 (0.999)	0.230 (0.028)*†
LPJ-GUESS	PFTs: 6 tree, 1 grass	cohort	photosynthesis, allocation, cross-PFT competition, cross-cohort competition	-7.290 (0.452)	0.056 (0.018)*	-7.379 (0.597)	-0.069 (0.027)*
LPJ-WSL	PFTs: 5 tree, 1 grass	PFT	photosynthesis, allocation, cross-PFT competition, cross-PFT competition	-7.829 (0.943)	0.252 (0.018)*†	-7.106 (0.964)	-0.020 (0.027)
JULES-TRIFFID	PFTs: 2 Tree, 2 grass, 1 shrub	PFT	Photosynthesis, allocation, cross-PFT competition	-8.633 (1.075)	0.411 (0.022)*†	-8.639 (0.952)	0.203 (0.033)*†

702

703 Manuscript Figures



704
705 **Figure 1:** Overview of the unified conceptual framework (gray boxes) for parallel analysis of
706 empirical data (blue boxes) and model output (red boxes). For ecosystem models, we describe
707 the latent climatic and ecosystem processes that are unobservable in paleoecological data and
708 differences among models in complexity. Complexity here is organized into three categories: 1)
709 diversity, ranging from a few plant functional types (PFTs) to many species; 2) demography,
710 ranging from ‘big leaf’ models with no explicit treatment of forest demography to models with
711 individual trees; and 3) ecophysiological processes. Changes in forest biomass emerge from
712 latent ecophysiological processes including gross primary productivity (GPP), net primary
713 productivity (NPP), net ecosystem exchange (NEE), and leaf area index (LAI).
714 Ecophysiological processes are controlled by model representation of higher-level vegetation
715 processes (Table 1). Latent model drivers, processes, and states (red boxes) result in estimates
716 of forest composition and biomass that can be compared to paleoecological data products (blue
717 boxes). Models vary in complexity due to design philosophy and tradeoffs between model
718 complexity and computational speed.

720

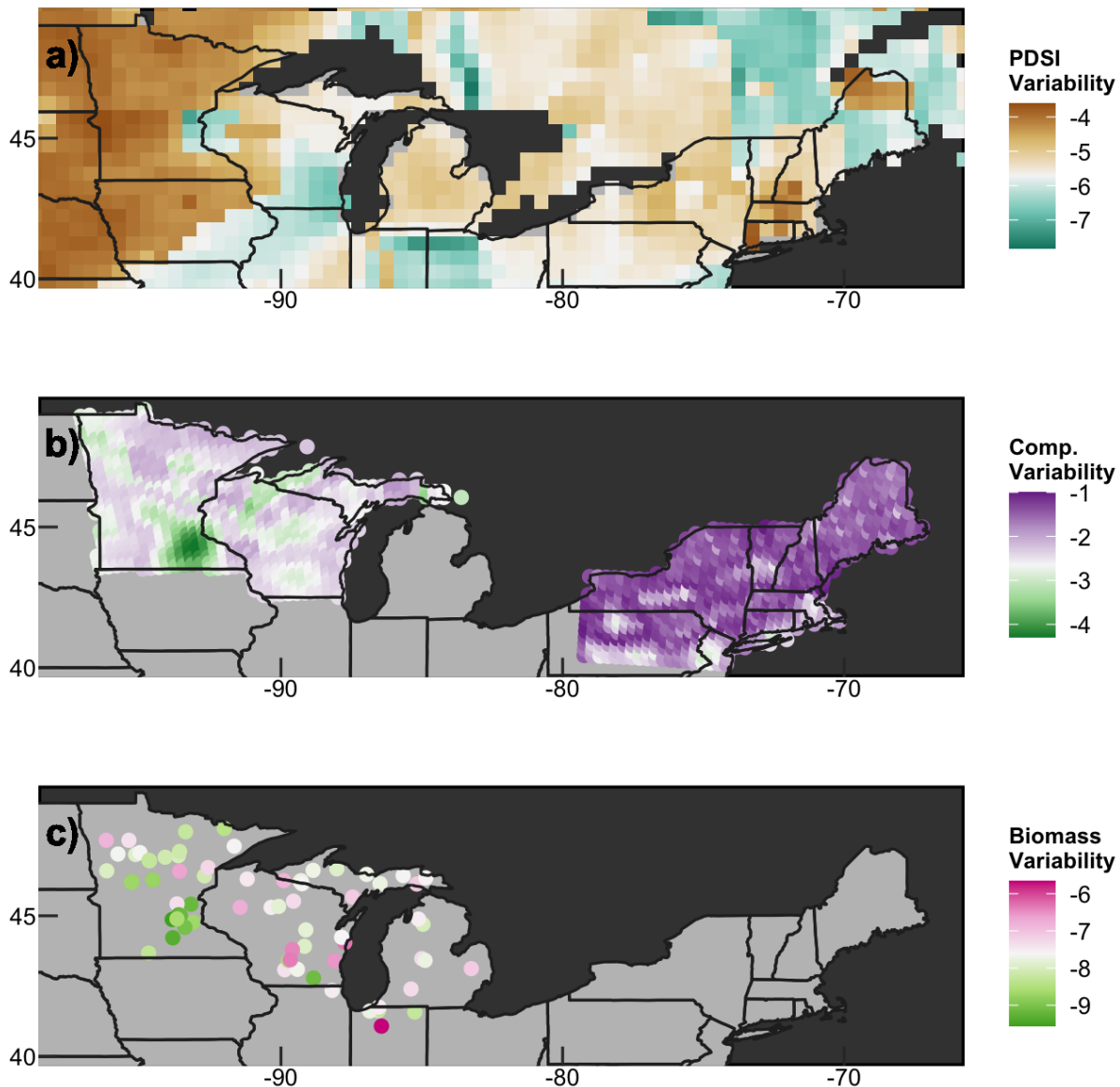
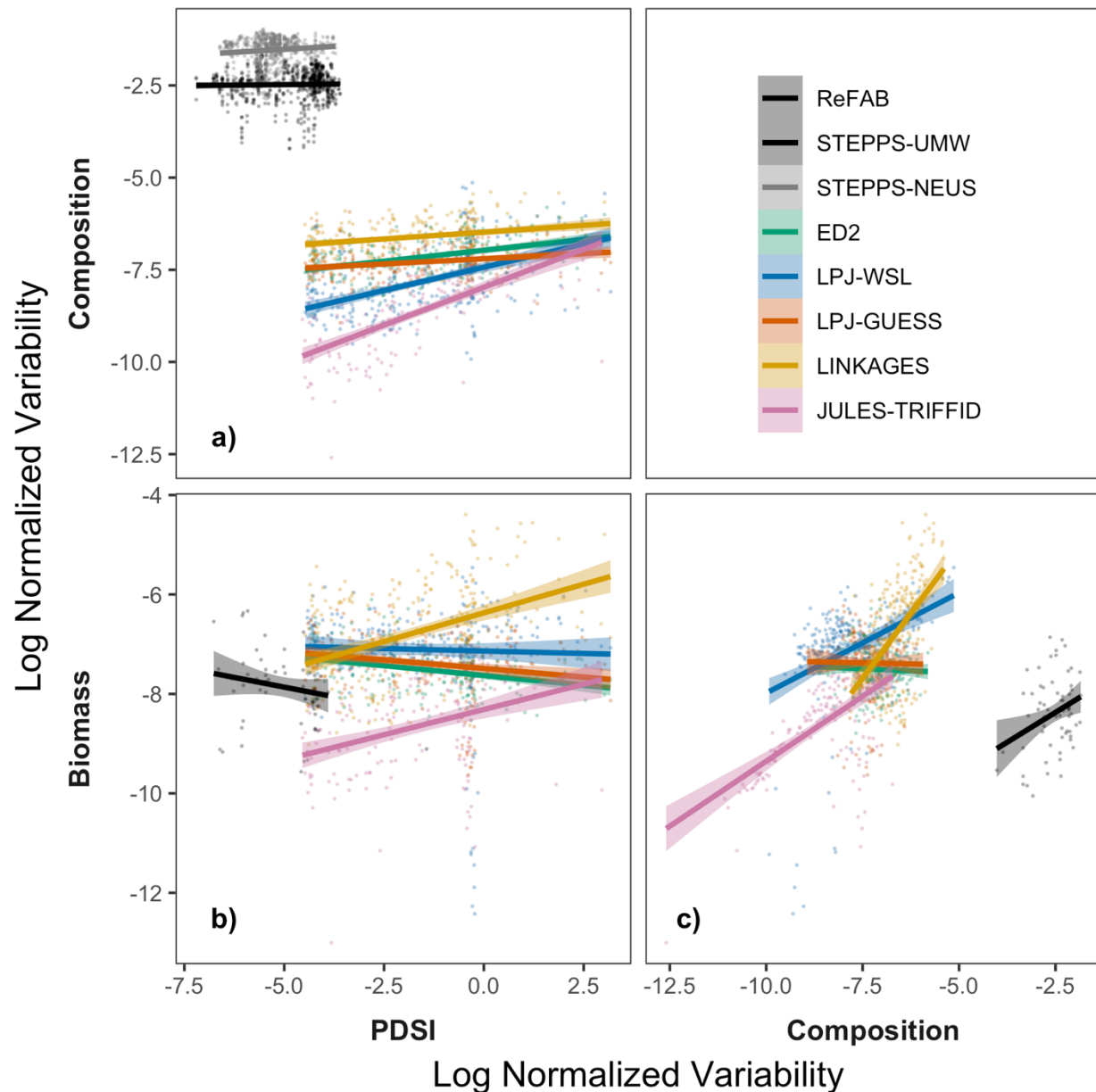


Figure 2: Spatial distribution of inferred temporal variability for 850 to 1850 AD for a) drought (PDSI) from the Living Blended Drought Atlas (44), b) forest composition from the STEPPS pollen-vegetation model (8, 24), and c) forest aboveground biomass from the ReFab pollen-biomass model (7). All variability estimates were divided by mean to facilitate inter-variable comparison (*Methods*). Spatial extents of compositional and biomass reconstructions are uneven across the study domain, as is the temporal extent of reconstructed drought variability (Supplemental Figure 1). Empirical comparisons of composition or biomass variability with drought variability are restricted to the common temporal extents for each location. In the log scale, negative values indicate locations with low variability whereas more positive values indicate high variability.

721
722
723
724
725
726
727
728
729
730
731
732
733

734



735

736

737

738

739

740

741

742

743

744

745

746

747

748

749

750

751

752

753

754

Figure 3: Inferred (black, gray) and simulated (colors) sensitivity of variability of forest composition and biomass to ecohydrological variability (PDSI) (a,b) and of biomass variability to compositional variability (c). Inferred variables suggest weak to no correlation (low sensitivity) between climate variability and ecosystem variability (composition and biomass). In contrast, ecosystem models generally simulate higher sensitivity of ecosystems to climate variability. Inferred compositional (STEPPS) and biomass (ReFAB) variability are positively correlated, while this relationship varied among models. In the log scale, negative values indicate locations with low variability whereas more positive values indicate high variability.

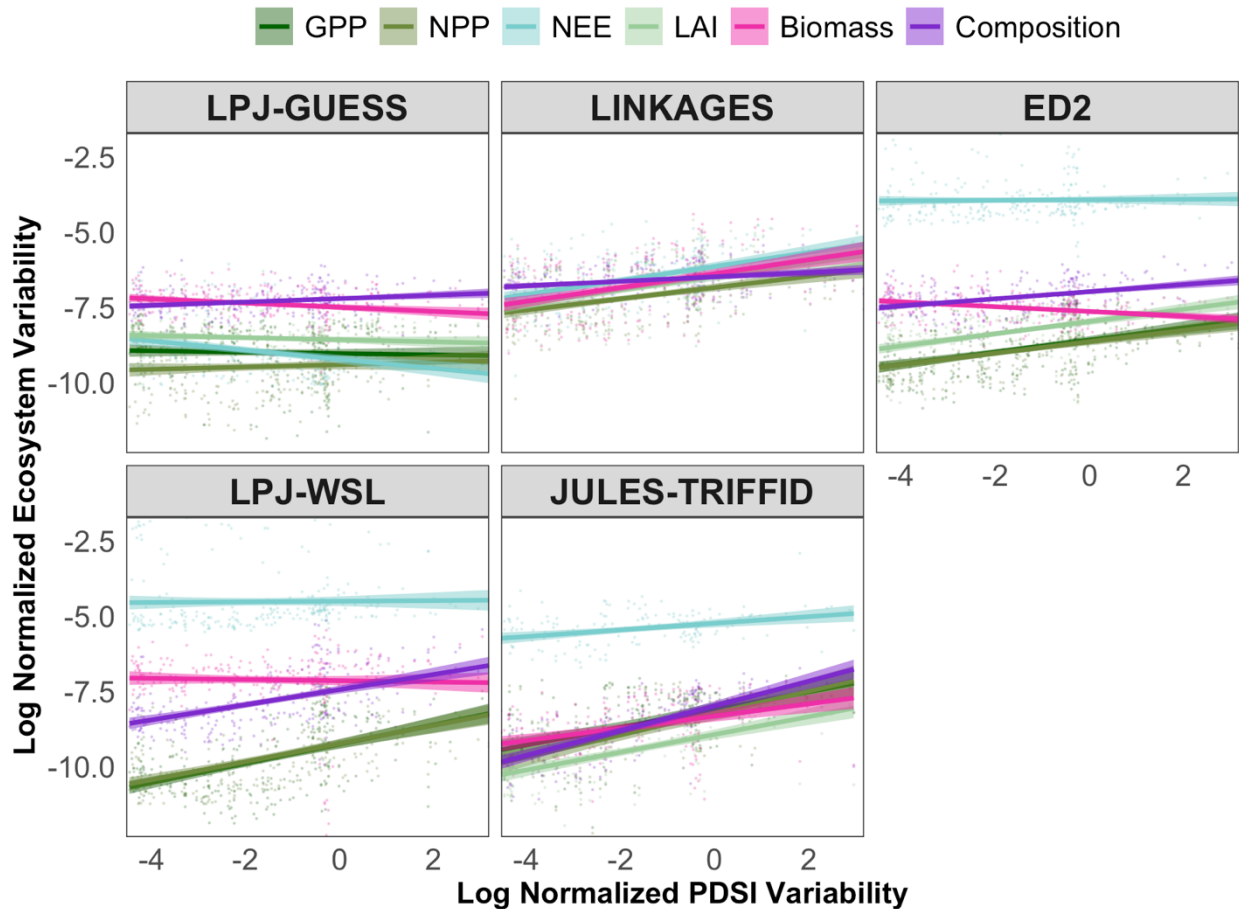


Figure 4: Diagnosing the observed and latent relationships among ecohydrological variability and variability in forest composition, structure, and function in five terrestrial ecosystem models. Models in the top row (LPJ-GUESS, LINKAGES, ED2) have individual- or cohort-level representation of demography whereas those in the bottom row (LPJ-WSL, JULES-TRIFFID) do not simulate demography. All models showed positive correlations between composition and drought variability, but some models showed positive biomass sensitivities (LINKAGES, JULES-TRIFFID) while others were negative (ED2, LPJ-WSL, LPJ-GUESS). In all models, composition sensitivity to hydroclimate variability was most similar to NPP whereas biomass sensitivity tended to mirror NEE. In the log scale, negative values indicate locations with low variability whereas more positive values indicate high variability.

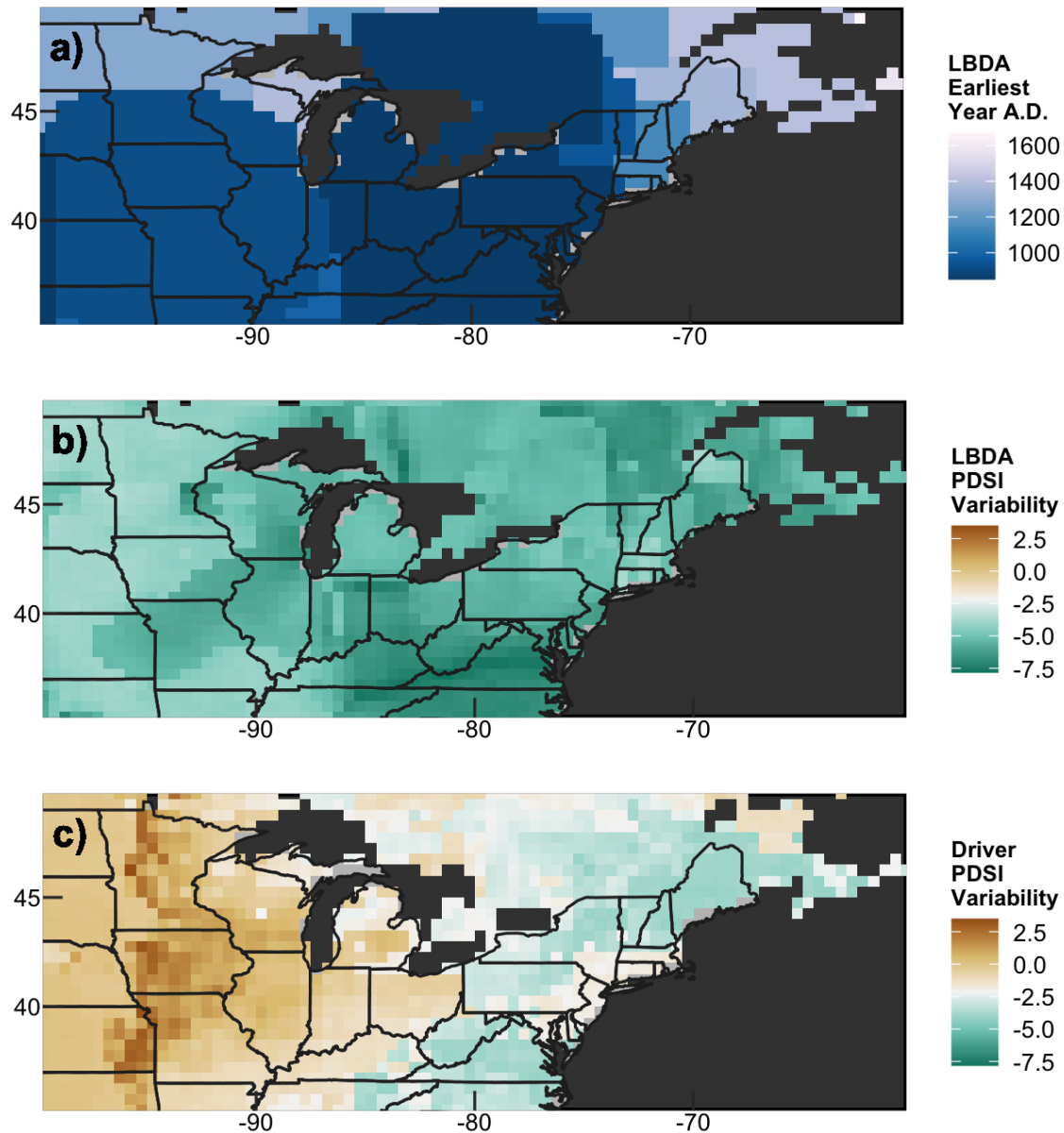
757 **Supplemental Tables**

758 **Supplemental Table 1:** Sensitivity of latent state variability to hydroclimate (PDSI) variability
 759 in ecosystem models and pollen data products. Sensitivity is presented as the mean and standard
 760 error slope from log-log regression; * indicates slopes significantly different from zero ($p < 0.05$).
 761 LINKAGES does not simulate GPP. LAI output was not available for LPJ-WSL.

Model	GPP	NPP	NEE	LAI	Biomass	Composition
Pollen					-0.156 (0.119)	0.026 (0.019)
ED2	0.201 (0.028)*	0.190 (0.025)*	0.008 (0.024)	0.203 (0.024)*	-0.079 (0.015)*	0.118 (0.017)*
LPJ-WSL	0.320 (0.033)*	0.301 (0.033)*	0.010 (0.034)		-0.020 (0.034)	0.252 (0.029)*
LPJ-GUESS	-0.022 (0.031)	0.038 (0.034)	-0.152 (0.031)*	-0.034 (0.022)	-0.069 (0.020)*	0.056 (0.015)*
LINKAGES		0.186 (0.027)*	0.232 (0.030)*	0.222 (0.031)*	0.230 (0.033)*	0.074 (0.016)*
JULES-TRIFFID	0.294 (0.051)*	0.365 (0.051)*	0.110 (0.028)*	0.295 (0.035)*	0.203 (0.038)*	0.411 (0.033)*

762

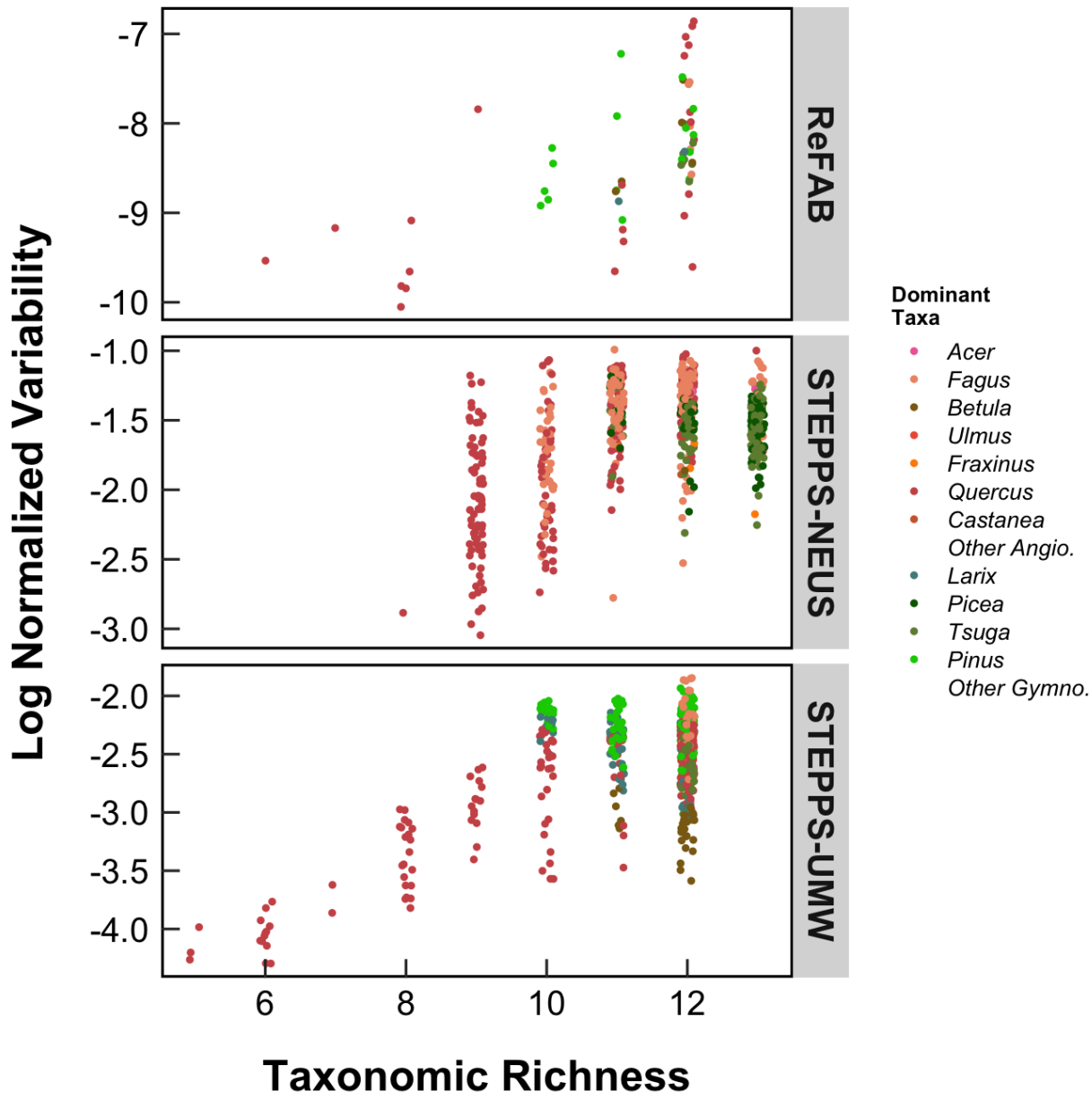
763 Supplemental Figures



764
 765 **Supplemental Figure 1:** Comparison of log normalized PDSI variability in empirically-inferred
 766 reconstructions from the Living Blended Drought Atlas (LBDA, 41, a, b) and model drivers (c).
 767 Due to the regional differences in the length of tree-ring chronologies available for PDSI
 768 reconstruction, the temporal extent of analyses involving LBDA drought is uneven across space.
 769 Overall, model drivers had greater PDSI variability than seen in the LBDA, but both datasets
 770 show greater variability in the western region of the study domain.
 771

772

1
2
3
4
5
6
7
8
9
10
11
12
13
14
15
16
17
18
19
20
21
22
23
24
25
26
27
28
29
30
31
32
33
34
35
36
37
38
39
40
41
42
43
44
45
46
47
48
49
50
51
52
53
54
55
56
57
58
59
60



Supplemental Figure 2: Relationship between taxonomic richness and log normalized biomass (ReFAB) and composition (STEPPS) variability in pollen-inferred datasets.

773
774
775
776